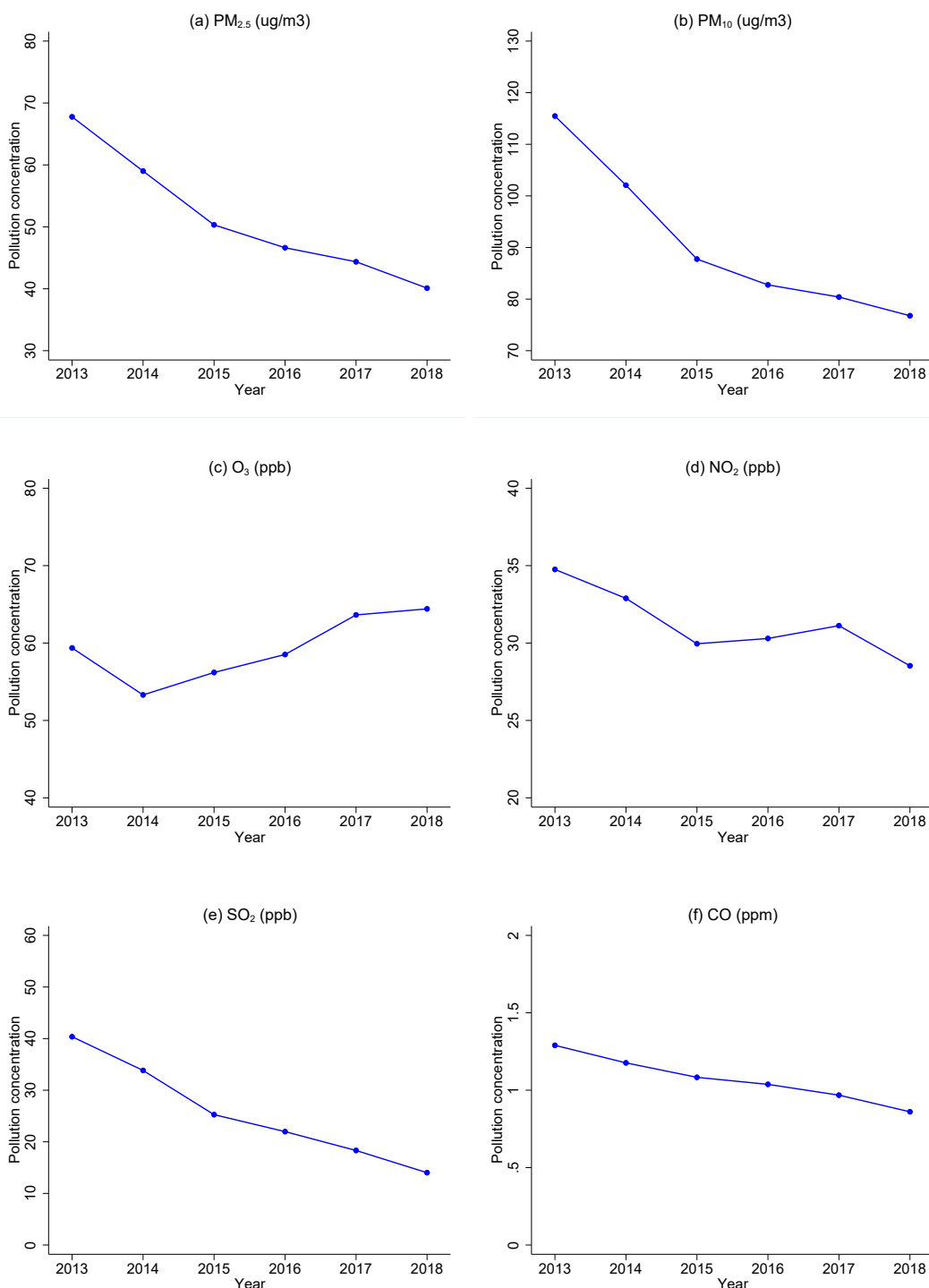


Online Appendix for

China's War on Pollution: Evidence from the First Five Years

Michael Greenstone, Guojun He, Shanjun Li, Eric Zou

Figure A.1. Concentration of Six Pollutants from Monitoring Stations



Notes: These graphs report annual concentrations for 6 pollutants average across all monitoring stations.

Pollution Trends Using Satellite-based Measures Appendix Figure A.2 compares the trends using the PM_{2.5} data from the real-time pollution monitoring system by China's Ministry of Ecology and Environment (MEE), and the satellite-based estimates based on van Donkelaar et al. (2016). Between 2013 and 2018, PM_{2.5} levels dropped by 27.7 $\mu\text{g}/\text{m}^3$, or about 41 percent from 2013 levels. The satellite-based estimates indicate a rise in PM_{2.5} from 2000 onward, followed by a remarkable drop-off beginning in 2013. Our calculation shows higher levels of PM_{2.5} from the monitoring data than the satellite-based estimates. We note this could be due to the remaining difference in spatial coverage between the two datasets, and/or uncertainties in both the satellite estimates and ground monitoring data, among other potential explanations. The van Donkelaar et al. (2016) estimates come at a spatial resolution of 10-by-10-km; thus, we cannot calculate levels of PM_{2.5} at the exact location of the monitors.

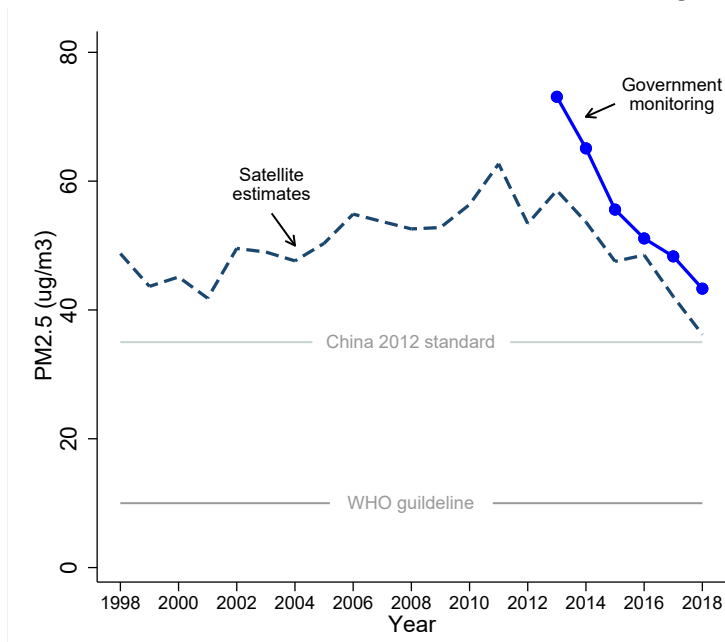
A potential concern with government-provided air quality data in China is manipulation (e.g. Ghanem and Zhang 2014). Appendix Figure A.3 presents a week-to-week comparison of the real-time PM_{2.5} data with independent monitoring by the United States in five major cities: Beijing, Chengdu, Guangzhou, Shanghai, and Shenyang. For all five cities, data provided by the MEE and the U.S. Embassy and consulates match quite well, both for absolute levels and the seasonal patterns of PM_{2.5}. Starting in 2013, both data sources show a clear decline in PM_{2.5} levels. In Appendix Figure A.4, we have also confirmed that MODIS column Aerosol Optical Depth values - one of the key inputs for measuring particulate pollution in van Donkelaar et al. (2019) - also show a downward trend starting 2013.

Spatial Heterogeneity in Pollution Trends To further explore regional differences in PM_{2.5} reductions, we estimate a linear trend in PM_{2.5} for each city using the monitoring data from 2015 when all cities had begun real-time air quality monitoring. We plot the city-specific coefficient estimates in Appendix Figure A.5. Panel (a) shows the average annual changes between 2015 and 2018 in PM_{2.5} by city, and panel (b) shows the percentage changes. We observe a striking PM_{2.5} decline in many cities of the country, including the area around Beijing, parts of the northeast, and parts of the west. Notably, the area around Beijing, one of the focal points of China's cleaning-up efforts, experienced a reduction of over 12 $\mu\text{g}/\text{m}^3$ per year during 2015-2018. We predict that, back in 2013, only 20 percent of Chinese cities (13 percent of the population) were in compliance with the government's 2012 ambient PM_{2.5} annual standard of 35 $\mu\text{g}/\text{m}^3$. In 2018, about 41 percent of the cities (29 percent of the population) met the standard. There is substantial heterogeneity in the magnitude of air quality improvements across different cities. While air quality improvement occurred almost across the entire nation, a handful of places, such as Linfen in Shanxi Province and Chizhou in Anhui province, experienced consistent increases in PM_{2.5}.

The rich spatial pattern shown in Appendix Figure A.5 raises the question of why air quality improved much faster in certain cities than in others. While it is beyond the scope of this paper to examine the causes underlying the spatial heterogeneity, we document several correlates of air quality improvement. Appendix Figures A.6 and A.7 report coefficient estimates from a cross-sectional regression of the PM_{2.5} reduction per year in level and in percentage, respectively, on city-level demographic and industrial characteristics during the 2011-2012 (baseline) period. We find that air quality improved more quickly during the 2015-2018 period in cities that were larger in population size and wealthier, as measured by GDP per capita. In addition, cities that had high concentrations of certain industries - such as the stone, clay, and glass-product manufacturing sectors - showed significantly larger pollution reductions. Cities with more coal mining activities and the waste recycling industry were less likely to experience such reductions.

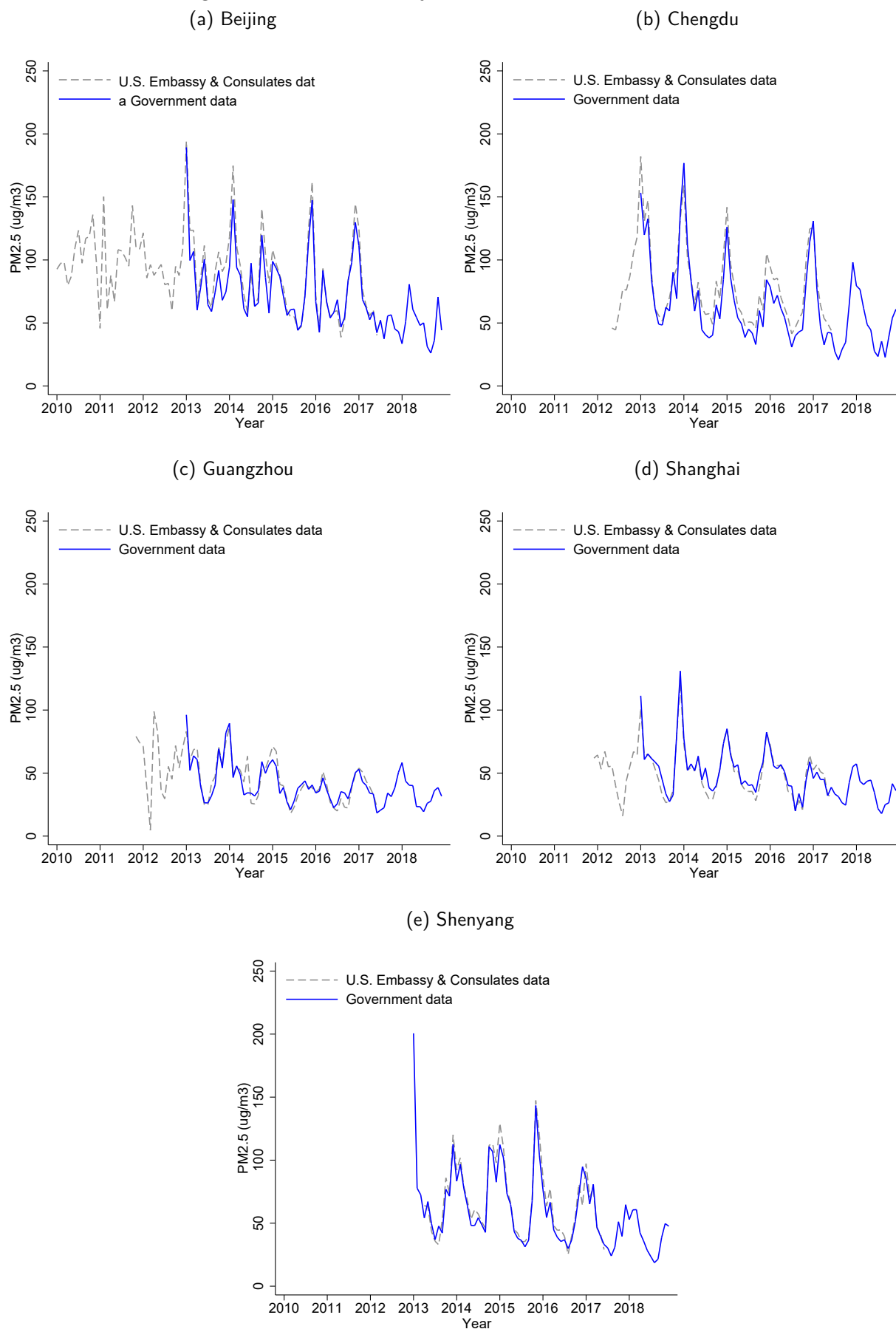
These correlations are not necessarily causal, and understanding the precise causes of the pollution reductions warrants further research. We only note that there have been a wide variety of policies that target air pollution and energy consumption, and sorting out the causal impacts of individual ones would be of great academic and policy interest. The impacts and effectiveness of these policies are the focus of Karplus et al. (2020) and Auffhammer et al. (2020) in the symposium.

Figure A.2. Trends in PM_{2.5} from Satellite and Motoring Stations



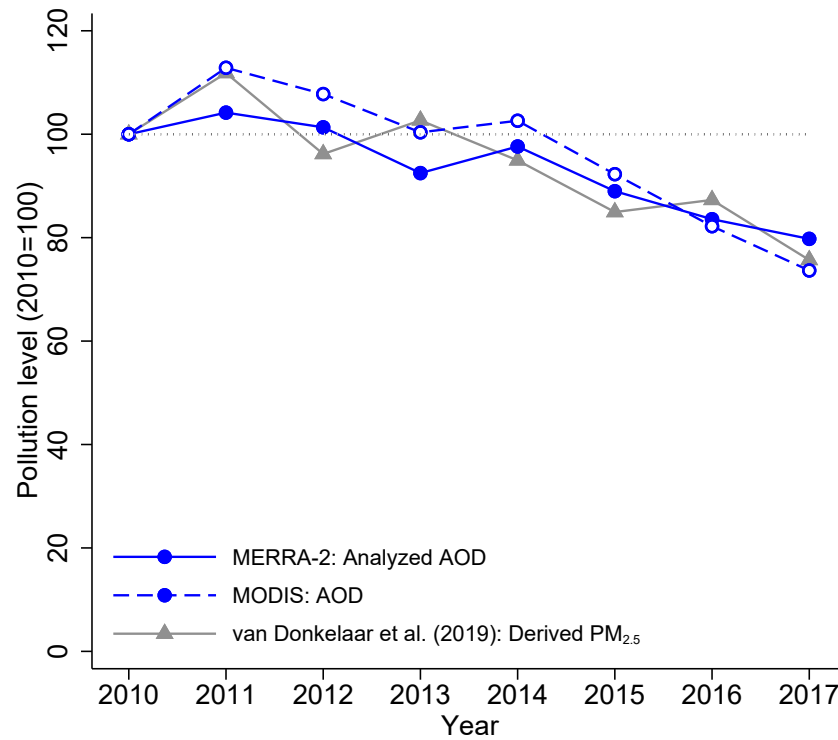
Notes: This graph reports annual PM_{2.5} concentration. The connected line is PM_{2.5} trend using the government monitoring data. Estimates are obtained from an OLS regression of city×daily PM_{2.5} concentration on calendar year indicators (omitting y2013) and city fixed effects. The values in the graph equal the coefficients on the year indicators plus the regression constant term. The dashed line is PM_{2.5} trend using satellite-based PM_{2.5} estimates from Van Donkelaar et al. (2019). In computing this trend, we restrict to a fixed set of grid cells that contain the location of ground monitoring stations as of 2018. “China 2012 standard” refers to The Ambient Air Quality Standards GB 3095-2012 Class-II region standard (residential, industrial, mixed-use, and rural areas).

Figure A.3. U.S. Embassy versus Government PM_{2.5} Data



Notes: This graph reports monthly PM_{2.5} concentrations for 5 cities where PM_{2.5} monitoring is independently carried out by the U.S. Embassy & Consulates.

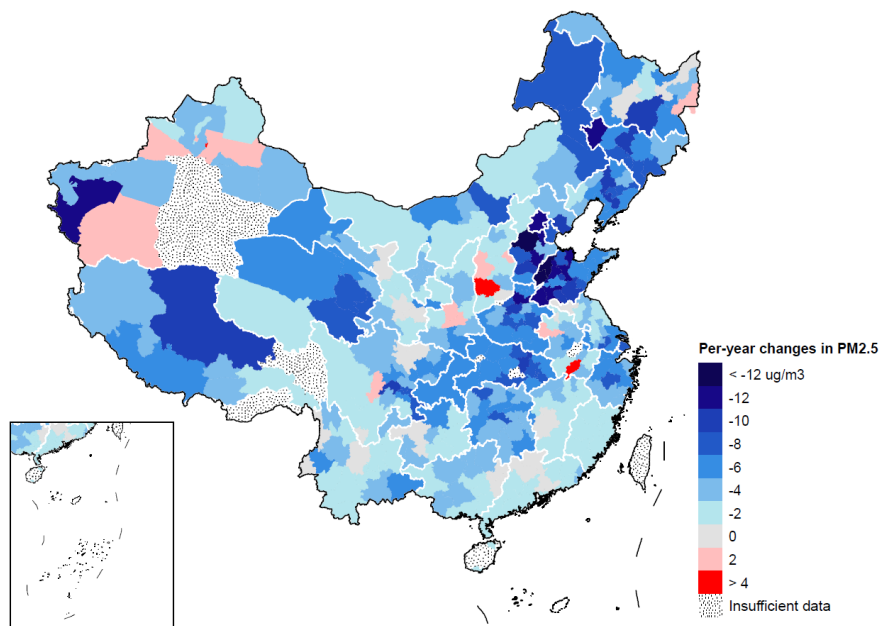
Figure A.4. Trends in AOD and Satellite-based PM_{2.5}



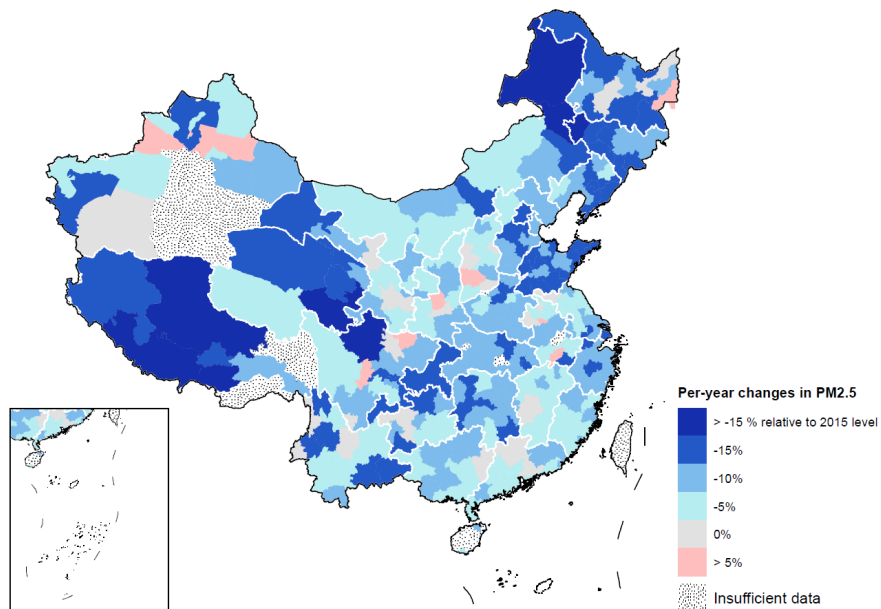
Notes: This graph reports trends in annual AOD measures and satellite-based PM_{2.5} estimates from Van Donkelaar et al. (2019). The AOD measures are from MERRA-2 and MODIS separately. The trends are based on OLS regression of city \times pollution measures on calendar year indicators (omitting y2013) and city fixed effects. The values in the graph equal the coefficients on the year indicators plus the regression constant term. The figure shows the changes in MERRA-2 and MODIS AOD over time - both based solely on satellite observations - compared with derived PM_{2.5} which is calibrated to ground monitoring. All three measurements suggest over 23% reduction in particulates pollution since 2010.

Figure A.5. Changes in PM_{2.5} by City, 2015-2018

(a) Level Change

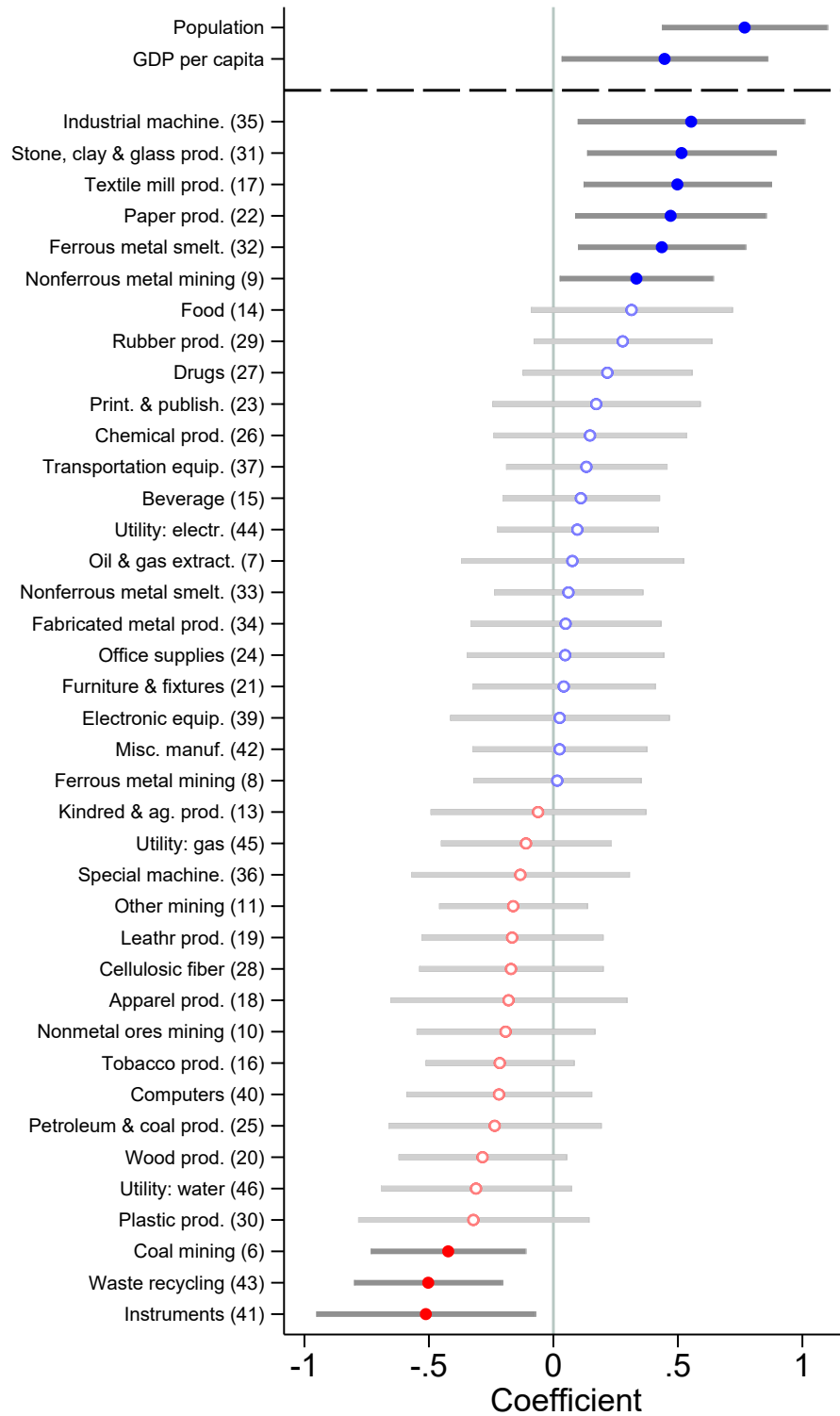


(b) Percentage Change



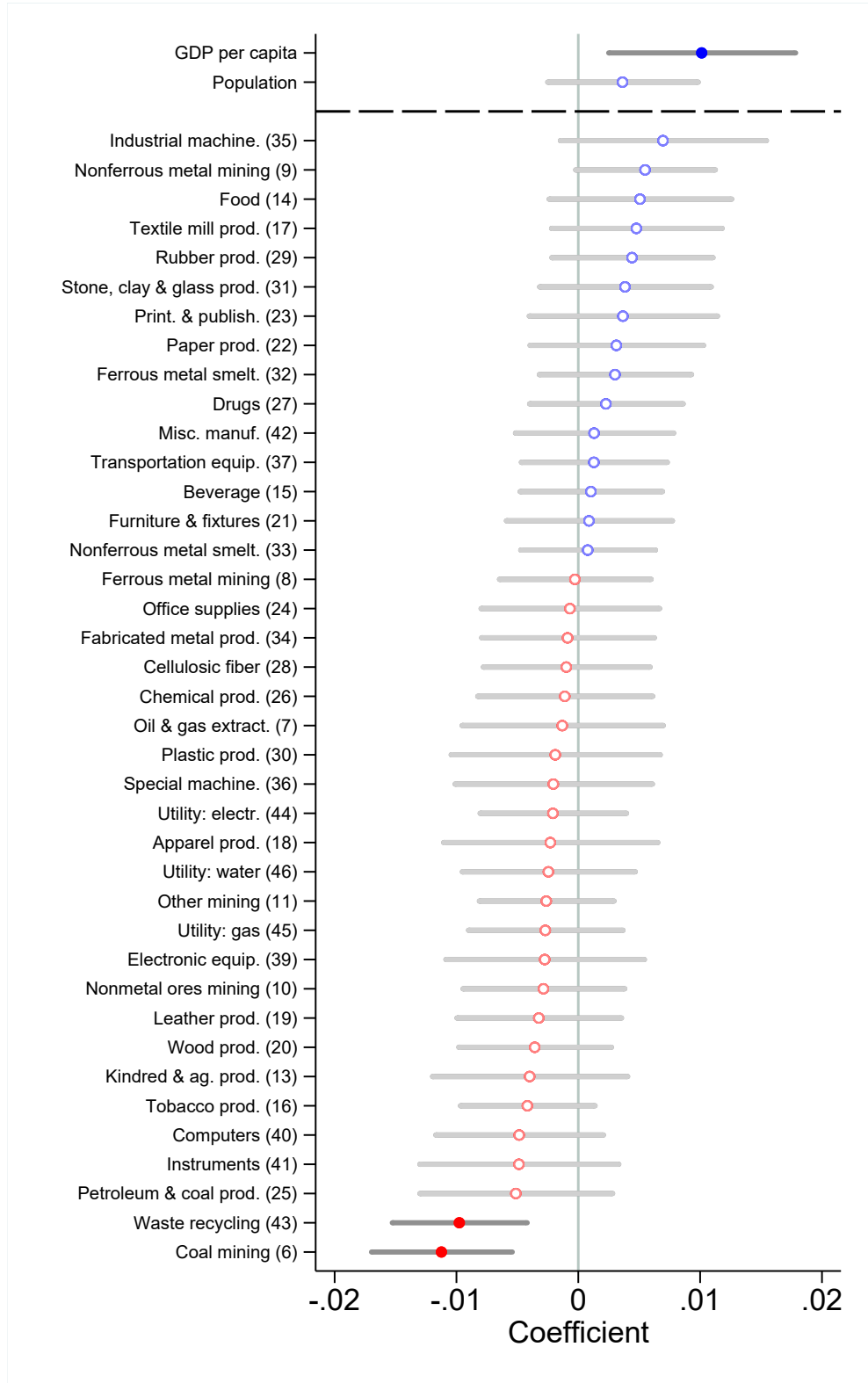
Notes: This maps plot the amount (top) and percentage changes (bottom) of PM_{2.5} per year for each city between 2015 and 2018. The estimates are obtained from separate OLS regressions (one for each city) of city × daily PM_{2.5} concentration on a linear year trend.

Figure A.6. Correlates of City-Level PM_{2.5} Reductions



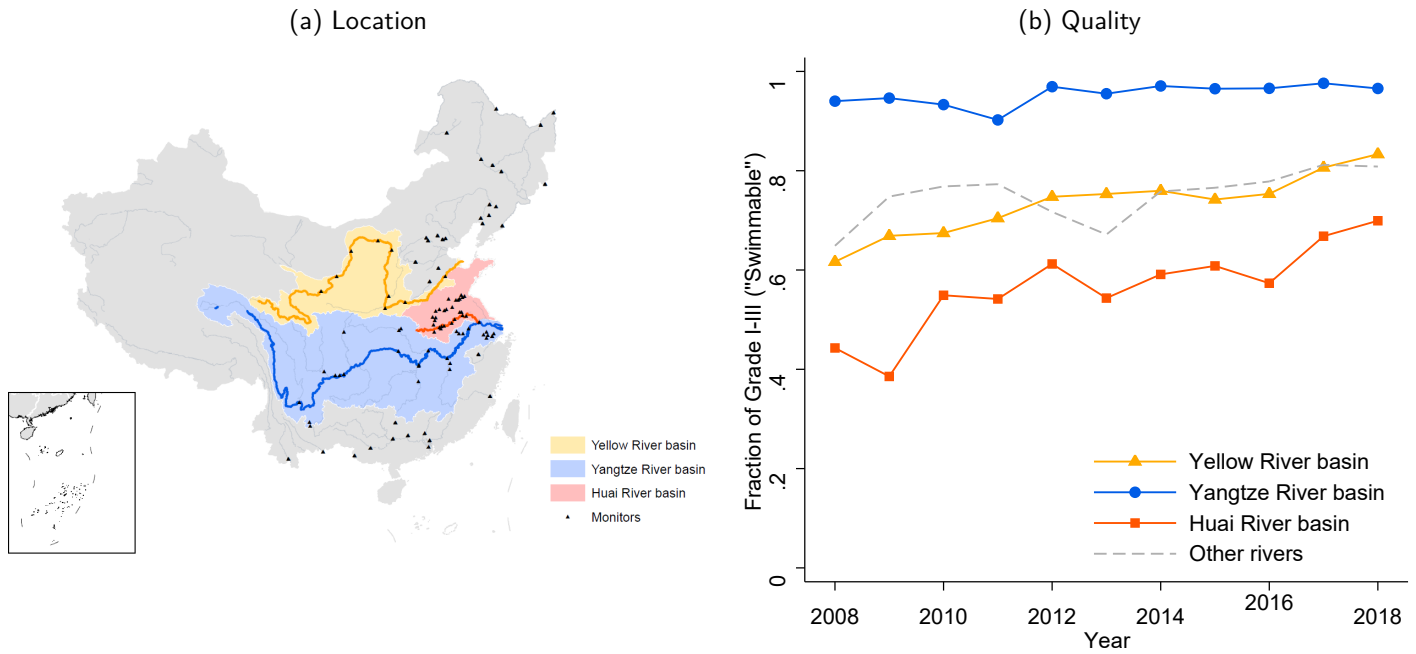
Notes: This graph reports correlates of city-level PM_{2.5} reduction between 2015 to 2018. To facilitate comparisons, all explanatory variables are normalized to have zero mean and unit standard deviation. Coefficient estimates from a single cross-sectional regression of city-level PM_{2.5} reduction per year on z-scores of baseline economic and industrial characteristics. For each 2-digit industry, the industry concentration is measured by the city's y2011-y2012 average industry revenue as a fraction of city's GDP. Solid dots in the graph indicate coefficient estimates that are individually statistically significant at the 5% level.

Figure A.7. Correlates of City-Level PM_{2.5} Reductions in Percentages



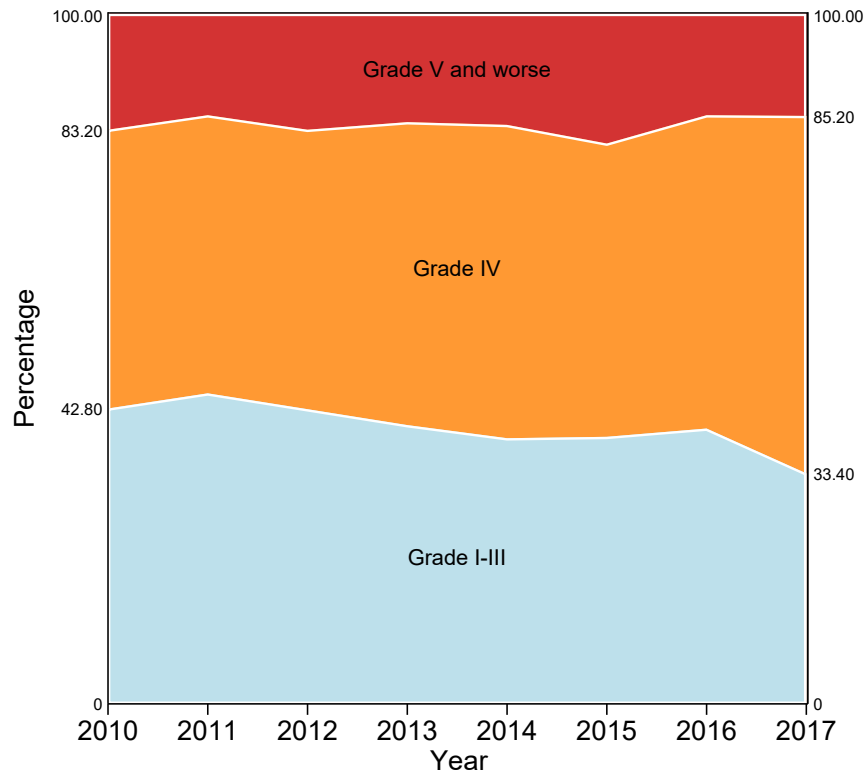
Notes: This graph reports correlates of city-level PM_{2.5} reduction in percentages between 2015 to 2018. To facilitate comparisons, all explanatory variables are normalized to have zero mean and unit standard deviation. Coefficient estimates from a single cross-sectional regression of city-level PM_{2.5} reduction per year on z-scores of baseline economic and industrial characteristics. For each 2-digit industry, the industry concentration is measured by the city's y2011-y2012 average industry revenue as a fraction of city's GDP. Solid dots in the graph indicate coefficient estimates that are individually statistically significant at the 5% level.

Figure A.8. Trends in Surface Water Quality at Major River Basins, 2010-2018



Notes: The map shows the location of the Yellow River basin, the Yangtze River basin, the Huai River basin, and other major rivers. Triangles represent water quality monitoring sites contained in the MEE's Major River Basins Water Quality Weekly Report. The right panel shows fraction of weeks in the year the water quality falls in the GB3838-2020 Grade I, II, and III categories (i.e., better than "swimmable"), averaged across monitors in the corresponding river basin.

Figure A.9. Trends in Ground Water Quality, 2010-2017



Notes: These statistics are from annual China Water Resources Bulletin. Underlying data are ground water quality sampled from 5,000 wells each year. The graph reports fraction of water samples that falls in the GB/T 14848-2017 Grade I-III ("residential use"), Grade IV ("residential use after treatment"), and Grade V categories ("not for residential use").